Weakened Vortex Shedding from a Rotating Cylinder

Sharul S. Dol

Abstract—An experimental study of the turbulent near wake of a rotating circular cylinder was made at a Reynolds number of 2000 for velocity ratios, λ between 0 and 2.7. Particle image velocimetry data are analyzed to study the effects of rotation on the flow structures behind the cylinder. The results indicate that the rotation of the cylinder causes significant changes in the vortex formation. Kármán vortex shedding pattern of alternating vortices gives rise to strong periodic fluctuations of a vortex street for $\lambda < 2.0$. Alternate vortex shedding is weak and close to being suppressed at $\lambda = 2.0$ resulting a distorted street with vortices of alternating sense subsequently being found on opposite sides. Only part of the circulation is shed due to the interference in the separation point, mixing in the base region, re-attachment, and vortex cut-off phenomenon. Alternating vortex shedding pattern diminishes and completely disappears when the velocity ratio is 2.7. The shed vortices are insignificant in size and forming a single line of vortex street. It is clear that flow asymmetries will deteriorate vortex shedding, and when the asymmetries are large enough, total inhibition of a periodic street occurs.

Keywords—Circulation, particle image velocimetry, rotating circular cylinder, smoke-wire flow visualization, Strouhal number, vortex shedding, vortex street.

I. INTRODUCTION

THE flow past a rotating cylinder provides a good diagnostic case for investigating vortex shedding from uneven opposing streets. Conceptually, the circulation due to the cylinder rotation induces asymmetry changes in the boundary layers and consequently the circulation convected into the shear layers. The flow field depends primarily on two parameters. The first is the velocity ratio,

$$\lambda = \frac{U_P}{U_\infty} \qquad (1)$$

where

$$U_P = \frac{\Omega D}{2} \qquad (2)$$

is the surface speed of the cylinder, U_∞ is the freestream velocity, Ω is the angular speed of the rotation and D is the cylinder diameter. The second is the Reynolds number,

$$Re = \frac{U_\infty D}{\upsilon} \qquad (3)$$

where υ is the kinematic viscosity of the fluid. To date, all studies have concentrated on the effects of the velocity ratio

Sharul S. Dol is with the Department of Mechanical Engineering, Curtin University, Miri, Malaysia (e-mail: sharulsham@curtin.edu.my).

while the Reynolds number effects have not been thoroughly investigated. It seems that the critical velocity ratio, which the suppression of periodicity occurs, is largely dependent on the Reynolds number. For example, [1] observed suppression at $\lambda \geq 0.6$ for $Re = 50$ while [2] observed suppression at $\lambda \geq 1.5$ for $Re = 2000$ and [3] observed suppression at $0.67 < \lambda < 0.72$ for $Re = 48000$ to 311000. There is a decay of the periodic vortex activity and an increase in the random modulation of the shedding process as λ increases [4], [5].

Badr et al. [6] investigated the unsteady flow past a rotating circular cylinder experimentally (flow visualization) and numerically for Reynolds numbers in the range $10^3 \leq Re \leq 10^4$ and velocity ratios, $0.5 \leq \lambda \leq 3.0$. The results show that the conventional periodic vortex shedding is altered substantially by the rotation. But they did mention that it was not possible to study the evolving periodic structure of the flow for a great time because of limitations of the visualization. However, this inadequacy is overcome by the present technique of particle image velocimetry (PIV), which is able to capture details of the vortex street thus providing more information to the vortex dynamics.

Vortex shedding patterns of a flow generated by a rotating circular cylinder were investigated experimentally at a Reynolds number of 2000. To the best of the author's knowledge, earlier investigations of vortex shedding process at moderate Reynolds number by a steadily rotating circular cylinder are the computational studies of [6]-[8] but most discussions are centered on the transient. Although [6] did include some experimental results, most of the findings discussed were numerically based. Massons et al. [2] did carry out flow visualizations around a rotating cylinder at $Re = 2000$. However, the shedding process was not clearly described as in those numerical studies. Dol et al. [9] did an experimental study (hot-wire anemometry and PIV) of the turbulent near wake of a rotating cylinder at a Reynolds number of 9000 and the results indicate that the periodic vortex shedding is suppressed for $\lambda \geq \sim 2.0$. The analysis was done mainly at $2 \leq x/D \leq 5$ (near wake region) to observe how convection speed of vortices, vortex spacing ratio, trajectory of vortex centroids and strength of shed vortices change with the velocity ratio. The interest was to examine the feature of Kármán vortex street at the suppression and they found that increased inequality of the two separated shear layers leads to weaker vortices in the near wake region.

The main objective of the present work was to study vortex shedding patterns at the base formation region. The interest was to examine the periodicity of vortex formation process and this analysis could provide an answer to weaker vortices found in the near wake region (i.e. the breakdown of Kármán vortex street). Estimation of vortex shedding frequency from

World Academy of Science, Engineering and Technology
International Journal of Mechanical and Mechatronics Engineering
Vol:7, No:10, 2013

the smoke-wire flow visualization was also included. Moreover, comparisons between the periodicity of vortex shedding patterns (or patterns of the vorticity contours) of present PIV results with the numerical results of [6] and [8] for Reynolds number of 1000, were discussed. In certain cases, numerical results from [7] were also included (i.e. *Re* = 1000, λ = 0.5 and *Re* = 3000, λ = 1.0).

II. EXPERIMENTAL DETAILS

The experiments were performed at the Boundary Layer Wind Tunnel Laboratory (BLWTL) of the University of Western Ontario (UWO) in a suction-type wind tunnel with a 1500 mm long working section and a 450 x 450mm^2 cross section, as shown in Fig. 1 (a). Hot-wire anemometry (HWA) measurements across the test section showed a uniform free-stream and a turbulence intensity of less than 1%. A smooth steel circular cylinder of nominal diameter D = 24mm was mounted horizontally in the midplane spanning the full width of the working section. A photograph of the set-up is shown in Fig. 1 (b). The cylinder aspect ratio was about 18.8 so that the statistical properties of the flow were effectively two-dimensional [2]. The blockage ratio was 5.3%, which is at the upper bound of the region of negligible blockage effects [10], [11], no correction was made for blockage effects. A definition sketch of the flow is given in [9].
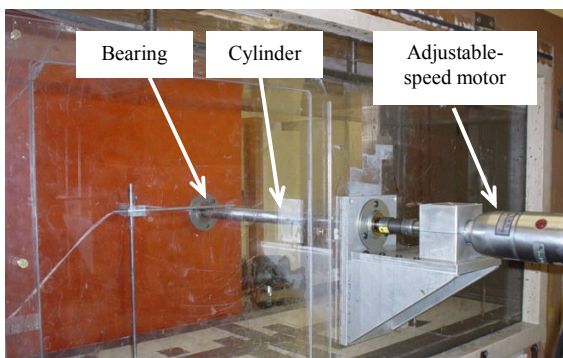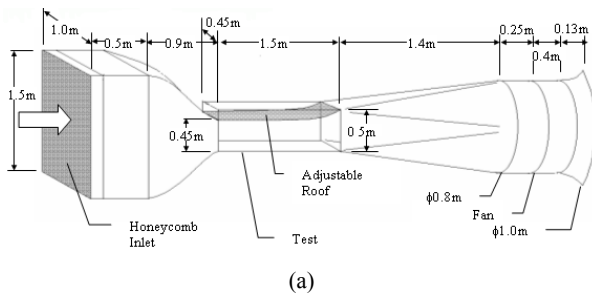

(a)

(b)

Fig. 1 (a) A Schematic representation of the wind tunnel (b) A photograph showing the mechanical set-up

Experiments (PIV and smoke-wire flow visualization) were performed at Reynolds number of 2000 and for speed ratios, λ, between 0 and 2.7. The experimental uncertainties were calculated using the methods described in [12], and are presented in Table I. Operating parameters for the PIV and smoke-wire flow visualization set-up and measurements can be found in [9].

TABLE I
UNCERTAINTY ESTIMATION

Variable	Error, ε			
D (m)	$\pm$ 0.0001			
U_∞ (m/s)	0.56 %			
f (Hz)	$\pm$ 0.15			
St	$\pm$ 0.006			
λ	0	1.0	2.0	2.7
	0	$\pm$ 0.007	$\pm$ 0.010	$\pm$ 0.020

III. RESULTS AND DISCUSSIONS

A. Stationary-Cylinder Results

Fig. 2 shows the evolution of smoke streaklines pattern for a complete cycle of a typical Kármán vortex shedding together with the instantaneous streamline patterns from PIV. Smoke in the form of streaklines which originate from the surface indicate the position of vortex sheets. It clearly can be seen that the vortex from the lower side of the cylinder grows in size until it occupies the entire recirculation region. At the maximum extent, the two shear layers interfere, eventually cutting off the supply of vorticity to the growing vortex, and causing the formed vortex to shed. A repeating pattern of counter-rotating vortices are shed continuously from each side of the body, forming rows of vortices in its wake. An instantaneous streamline plot in the reference frame of the cylinder shows a periodic fluctuation.

The visualizations also provide an estimation for the vortex shedding frequency. To complete a cycle, the formation of a vortex and its interaction in the base region is tracked until it is fully shedded downstream. This approach is only approximate, but does help in interpreting the more precise hot-wire anemometry (HWA) results, especially at higher λ. The average dimensionless vortex shedding frequency *f* is equal to 0.105, where

$$f = \frac{1}{T} \qquad (4)$$

and *T* is the dimensionless period of vortex shedding that is defined as

$$T = \frac{U_\infty t}{r} \qquad (5)$$

where *t* and *r* are the actual time and radius of the cylinder respectively. The non-dimensional shedding frequency (Strouhal number, $St = fD/U_\infty$) is related to *f* by

World Academy of Science, Engineering and Technology
International Journal of Mechanical and Mechatronics Engineering
Vol:7, No:10, 2013

$$St = 2f \qquad (6)$$

In this particular case, St is about 0.210 compared to 0.202 obtained via HWA. This value is in good agreement with [13]-[15] for a stationary circular cylinder case at this range of Reynolds number. Chew et al. [8] obtained St of 0.206.

Fig. 3 shows the vorticity contours taken at different times during half a cycle of vortex shedding. As expected, comparisons between the present experimental results and numerical results of [8] reveal a generally good agreement. Whilst the vortex on one side is being shed, the one on the other side is forming (an alternate vortex shedding phenomenon). The figures show a typical Kármán vortex shedding pattern of alternating vortices with the same strength advancing downstream. Although [8] did not measure the strength of vortices, this observation could be inferred from their figures (i.e. level of the vorticity contours).
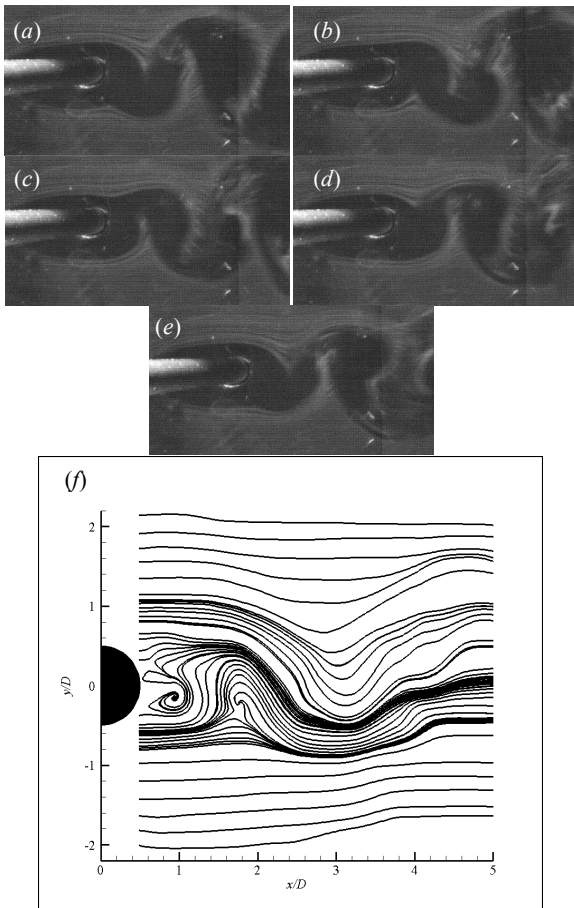

Fig. 2 Evolution of smoke pattern for a complete cycle of a typical Kármán vortex shedding for $\lambda = 0$, (a) T0 (b) T0+ 2.60 (c) T0+ 5.20 (d) T0+ 7.80 (e) T0+ 9.53 (f) instantaneous streamline patterns
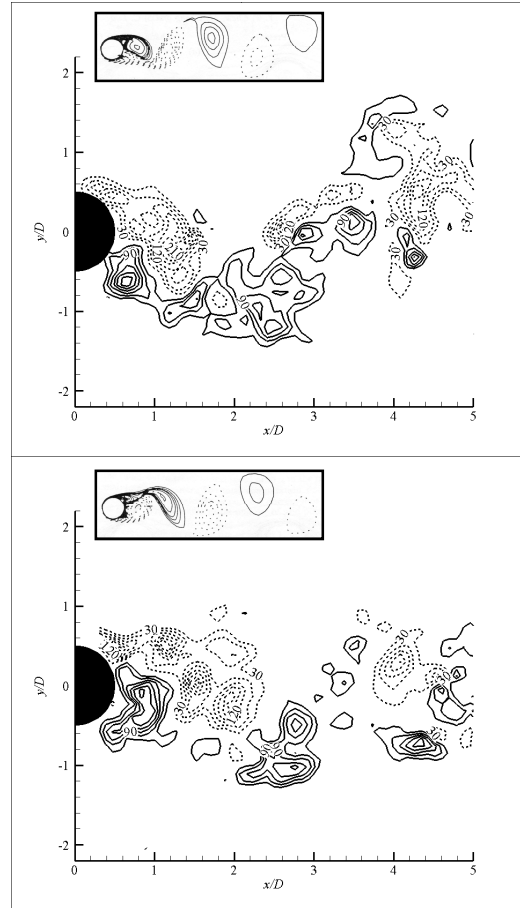

Fig. 3 Vorticity contours taken at different times during half a cycle of vortex shedding for $\lambda = 0$. Dashed (solid) lines represent constant negative (positive) vorticity values with a constant increment of ± 30 units, with the weakest contour level shown being ± 30, in this and subsequent figures. Corresponding numerical result by [8] is shown in bracket

B. Rotating-Cylinder Results

For $\lambda = 0.5$, the vortex phenomenology is similar to that for the non-rotating case. The clockwise and counter-clockwise vortices show an almost symmetrical process about the wake centerline. More details about the wake periodicity and investigation of the vortex street at this particular velocity ratio can be found in [16]. Where comparison is possible, the results of the present experiments are found to be in good agreement with the numerical results of [6], [8].

One interesting feature that is found at this velocity ratio is the appearance of a companion vortex upstream of the main vortex at the lower side of the cylinder as shown in Fig. 4. It appears as a small vortex, which has opposite vorticity to the main vortex. It is believed that the opposing motion between the moving wall and the counter-clockwise vortex very close to the surface on the lower side of the cylinder generates the small companion vortex. Both [6], who refers to secondary eddies and [8] observed a companion vortex, albeit these were reported for the transient (start-up) stage. In the present results, the companion vortex appears periodically and concurrently with the main lower (counter-clockwise) vortex.

World Academy of Science, Engineering and Technology
International Journal of Mechanical and Mechatronics Engineering
Vol:7, No:10, 2013

It thus appears that both structures are shed simultaneously. In this process, these two vortices can interact directly, and can cause the observed net reduction of the strength of the shed counter-clockwise vortex through mixing. However, the presence of the companion vortex can interfere with the net circulation production at the separation point, which can also cause a net reduction in the main clockwise vortex strength. Chang and Chern [7] also mentioned about the appearance of this companion vortex (they refer to intermediate vortex) at λ = 0.5 next to the cylinder in the lower wake, which subsequently coalesces with the newly-formed upper vortex to form the shedding clockwise vortex.
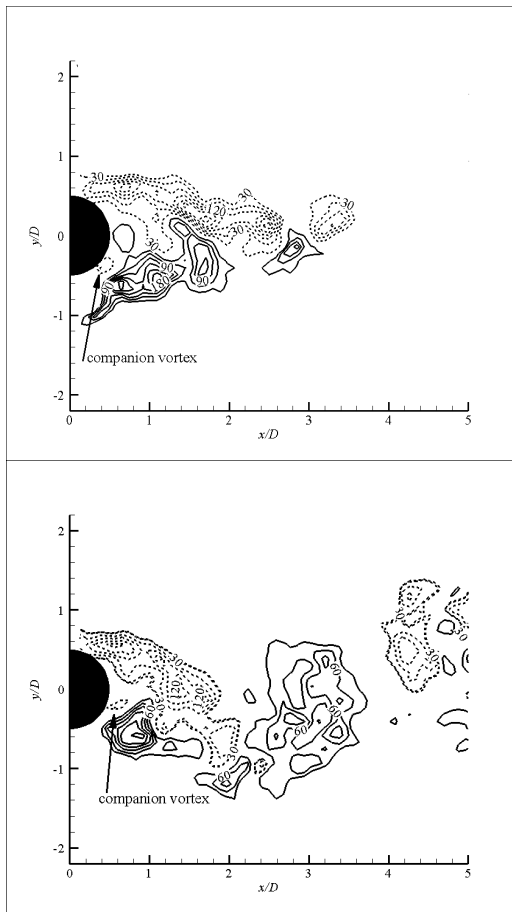
Fig. 4 Instantaneous vorticity contours showing a companion vortex at λ = 0.5

Fig. 5 shows the smoke patterns for a complete cycle of a vortex shedding together with the streamline patterns for λ = 1.0. The size of the vortices is smaller and the corresponding wake formation area has decreased markedly when compared to flow patterns for smaller λ. However, the clockwise and counter-clockwise vortices are similar in size, indicating insignificant vortex behavioral change due to cylinder rotation. Kármán vortex street is still visible in the wake. The average complete cycle of vortex shedding for the clockwise and counter-clockwise vortices corresponds to St = 0.256.

Shedding frequency obtained from HWA is 0.248 [16]. St obtained by [8] is 0.230. An instantaneous streamline plot in the reference frame of the cylinder shows a highly regular fluctuation as well as the upwards deflection. They match reasonably well with the steamline patterns and visualizations of [6].
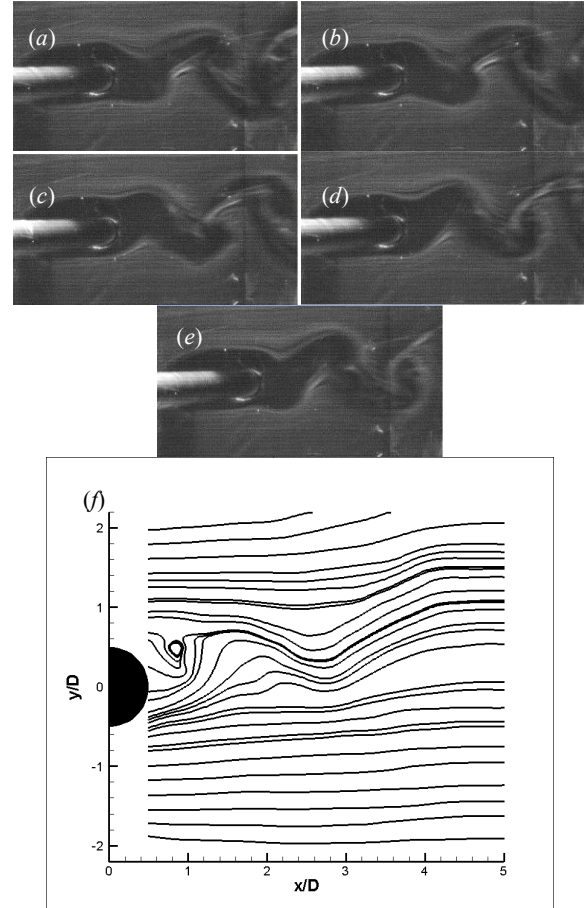

Fig. 5 Evolution of smoke pattern for a complete cycle of a typical Karman vortex shedding for λ = 1.0, (a) T_0 (b) T_0+ 1.73 (c) T_0+ 4.33 (d) T_0+ 6.07 (e) T_0+ 7.8 (f) instantaneous streamline patterns

Fig. 6 shows the instantaneous vorticity contours during a cycle of vortex shedding for λ = 1.0. The region at which vortices are formed is shifted in the direction of rotation. The companion vortex associated with the main vortex on the lower side of the cylinder is also clearly visible. This companion vortex still appears periodically. This phenomenon is also present in the results of [7], [8]. The strength of the main counter-clockwise vortices is only about 40% of the initial circulation at this velocity ratio (when compared to the stationary case). The influence of this companion vortex appears to be the reduction of circulation of the main counter-clockwise vortex perhaps by vorticity cancellation. Thus, it can be inferred that the reduction in circulation for the counter-clockwise vortices is due primarily to this interference in the base region. The simulations of [8] for λ =

World Academy of Science, Engineering and Technology
International Journal of Mechanical and Mechatronics Engineering
Vol:7, No:10, 2013

0.5 suggested that the companion vortex strengthened the upper (clockwise) main vortex. This latter mechanism appears incompatible with the present observations since: (i) the upper vortex is weaker than the lower (counter-clockwise) vortex, and (ii) there is no evidence of strengthening of the upper vortex.
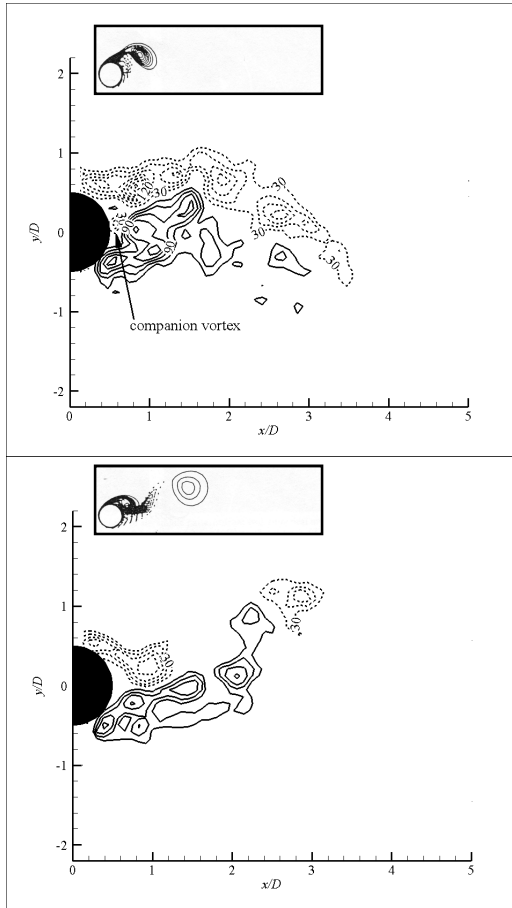

Fig. 6 Instantaneous vorticity contours during a cycle of vortex shedding for $\lambda = 1.0$. Corresponding numerical result by [8] is shown in bracke

For $\lambda = 1.5$, the asymmetry of the flow becomes more apparent. A companion vortex could not be identified at this velocity ratio. The clockwise and counter-clockwise vortices still appear to convect with the same speed. This implies that an inequality of the strength of the separated shear layers does not affect the occurrence of the periodic Kármán vortex street although the streamline topology is highly distorted due to the lack vortex activity in the wake, which agrees with the analysis of [17]. In contrast, [7] found that vortices in the lower wake are completely inhibited, which, however, does not necessarily imply the deterioration of the Kármán vortex structure in the wake.

Fig. 7 shows the evolution of smoke pattern for a complete cycle of a vortex shedding together with the streamline patterns for $\lambda = 2.0$. The estimation of Strouhal number is about 0.330, whereas St = 0.244 is obtained by [8].

The increment of Strouhal number is largely contributed by the large reduction in mean separation between the upper and lower vortices, resulting in early roll up and shedding times.

An instantaneous streamline plot in the reference frame of the cylinder shows unobvious fluctuating travelling wave. Generally, as λ increases the vortex cores are increasingly deflected in positive lateral direction and the separation between upper and lower vortices becomes smaller. The upper separation is advanced because the opposite moving surface advances the separation while the lower separation is delayed because moving surface energizes the fluid to overcome the adverse pressure gradient [5]. The rate of deviation from the non-rotating case is higher for the lower vortices as the velocity ratio increases [8].
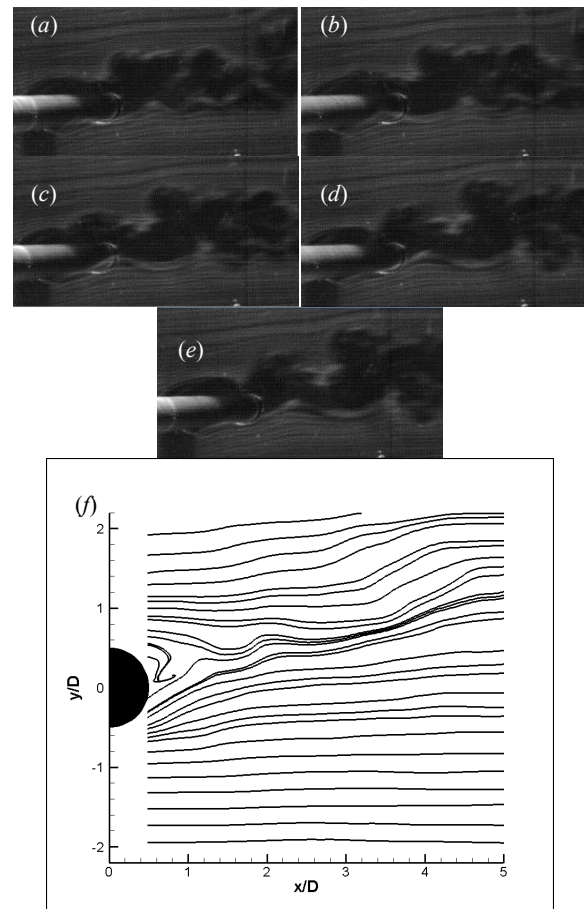

Fig. 7 Evolution of smoke pattern for a complete cycle of a vortex shedding for $\lambda = 2.0$, (a) T_0 (b) $T_0 + 1.73$ (c) $T_0 + 3.47$ (d) $T_0 + 5.2$ (e) $T_0 + 6.07$ (f) instantaneous streamline patterns

Fig. 8 shows the instantaneous vorticity contours for $\lambda = 2.0$. Despite the more pronounced wake distortion than at lower λ, a weak but regular vortex street is still observed. Both [6] and [8] found that at this rotational rate the shedding of vortices from the two shear layers appears to be regular and alternate, similar to the $\lambda = 0.5$ and 1.0 cases discussed earlier. But they did mention that after the start-up transient period, the amplitude of streamlines waviness decreases. There is a

World Academy of Science, Engineering and Technology
International Journal of Mechanical and Mechatronics Engineering
Vol:7, No:10, 2013

difference in vorticity strength between the vortices shed from the upper and lower sides of the cylinder and the increase in λ tends to suppress the process of positive (lower) vortex formation behind the cylinder [7], [8]. However, the present results clearly show the formation of vortices at both the upper and lower sides of the cylinder. More significantly and in contrast to the simulation results, the lower shed vortices have more circulation than the upper ones.

Unlike the classical shedding process, the vortices are not completely shed from the base of the cylinder. There are bound vortices at the base on the upper and lower sides of the cylinder and only part of the circulation (i.e. part of the vortex) is shed during each cycle. The bound vortex would thus interfere with the separation streamline at the surface of the cylinder and reduce the net rate of circulation flux, resulting in weaker vortices.

Although alternate vortex shedding appears, it is difficult to observe Kármán vortex street in the wake. Fig. 8 shows the distorted street, which at certain points, the positions of clockwise and counter-clockwise vortices are interchanged with the former one appears at the lower layer and vice versa. It seems that the counter-clockwise (clockwise) vortex cuts-off part of the clockwise (counter-clockwise) vortex at the base region, initiating probably the alternate vortex shedding process with the counter-clockwise vortices being the stronger ones. This observation triggered further investigation concerned with instability of vortex, many of which were discussed by [9]. Many investigators [2], [5]-[8] have reported that the shedding was favored from the upper cylinder surface where the free-stream and the rotation are opposite, but none have measured the circulation in the shed vortices. It was anticipated that weakening in the shed vortices was due to the vortex decay. Moreover, no companion vortex was formed at this velocity ratio. Thus, there must be another mechanism that causes this reduction.

It has been mentioned before that surface velocity of the cylinder reinforces the vorticity in the vortex (upper side) whereas the surface velocity of the cylinder diminishes its vorticity (lower side). However, [4] introduced an interesting but valid concept of a "relative Reynolds number", which seems to counteract that previously mentioned. When the surface is traveling with the free-stream velocity, the transition can be expected to be delayed, and conversely. The boundary layer behavior can then be correlated with the relative Reynolds number and a qualitative estimation of the relative portions of laminar and turbulent boundary layer and total length of boundary layer can be obtained. Due to the opposing motion between the wall and the free-stream, the upper relative Reynolds number increases, and conversely. This signifies a longer attached boundary layer on the top than on the bottom. At higher rotational speeds, a greater portion of the upper boundary layer becomes turbulent and therefore more re-attached.
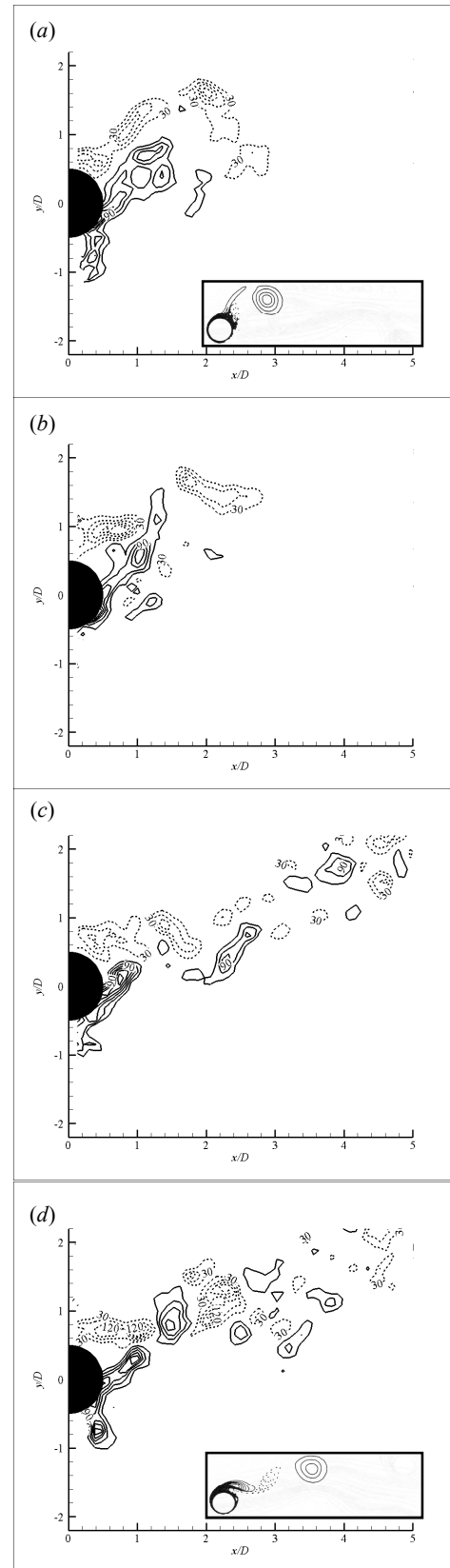

Fig. 8 Instantaneous vorticity contours for $\lambda = 2.0$. Corresponding numerical result by [8] is shown in bracket.

World Academy of Science, Engineering and Technology
International Journal of Mechanical and Mechatronics Engineering
Vol:7, No:10, 2013

Since at this velocity ratio ($\lambda = 2.0$), vortex cut-off is the responsible mechanism for the shedding process, the locations for the flow separation are important. When the counter-clockwise vortex cuts the clockwise vortex (interrupts the flow of circulation), most of the circulation is believed to be pulled upstream by the moving surface and disappearing. Only a small fraction of the circulation is shed. On the other hand, when the clockwise vortex cuts the counter-clockwise vortex, a major fraction of the circulation is shed resulting in a counter-clockwise vortices being stronger. Badr et al. [6] reported that some of the bounded vortices migrated to the frontal part of the cylinder and disappeared. The shed vortices contain significantly lower circulation, suggesting that a much smaller fraction of the circulation is shed when compared to $\lambda \leq 1.5$. It is quite clear that the increase of λ tends to suppress the process of periodicity behind the cylinder.

Fig. 9 shows the instantaneous vorticity contours for $\lambda = 2.7$. The pattern of alternate vortex shedding has disappeared. Clockwise and counter-clockwise vortices are shed at the same time. In other words, the positive vorticity shed engulfs and neutralizes the negative vorticity. The attached or bound vortex is still present. Chew et al. [8] showed that a periodic flow pattern did not develop for $\lambda = 3.0$. The present results disagree with the numerical results of [6] that found the vortices are shed only from the upper shear layers. In the present work, the clockwise and counter-clockwise vortices are still being shed but intermittently. The shed vortices are insignificant in size and forming a single line of vortex street. Kármán vortex street ceases to develop. Fig. 10 shows the corresponding smoke patterns that confirm the suppression of the periodicity. Physically, the upper shear layer is too weak to couple with instabilities in the bottom shear layer. It is interesting to note that the vortices in the upper half wake that are more significantly weakened than those from the lower wake. These results are, therefore, seen to be consistent with the stability criterion for the formation of a vortex street, as given by [17] and [18].
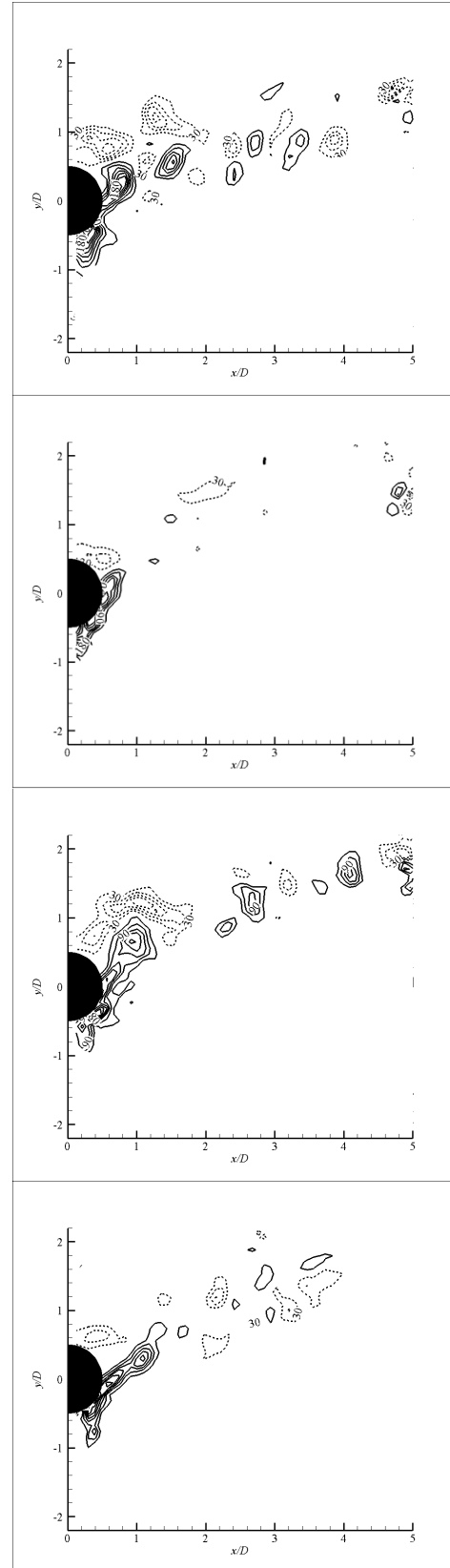

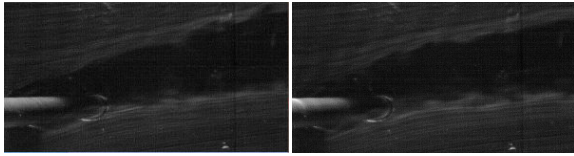Fig. 9 Instantaneous vorticity contours for $\lambda = 2.7$.

World Academy of Science, Engineering and Technology
International Journal of Mechanical and Mechatronics Engineering
Vol:7, No:10, 2013

Fig. 10 Smoke patterns taken for $\lambda = 2.7$.

IV. Conclusion

PIV and smoke-wire visualizations were made in the wake of a rotating circular cylinder in a uniform freestream with the objective of describing the patterns of the vortex shedding (formation and evolution) up to suppression of the periodic vortex street at high velocity ratios. The results obtained in the present study establish that shedding of Kármán vortices in a rotating circular cylinder-generated wake is modified by rotation of the cylinder. While periodic vortex shedding appears, the results show that the patterns are generally comparable to the reported numerical results.

Alternate vortex shedding is highly visible when $\lambda < 2.0$ although the strength of the separated shear layers differ due to the rotation of the cylinder. As opposed to the earlier numerical results, the clockwise vortices those are more significantly weakened than the counter-clockwise vortices. For $\lambda = 0.5$ and 1.0, the reduction in circulation is possibly due to interaction (mixing) between the main vortex and the companion vortex, which associates periodically with the main counter-clockwise vortex. This companion vortex also disrupts the net circulation production. At higher velocity ratios, re-attachment of the turbulent boundary layer may lead to less circulation in the shed vortices. Alternate vortex shedding is weak, distorted and close to being suppressed at $\lambda = 2.0$. Since the cylinder rotation affects the flow separation points (upper and lower sides of the cylinder), the shedding process is modified and mostly due to the vortex cut-off process, which makes the counter-clockwise vortices being the stronger ones. The bound vortices then interfere with the flow separation thus reducing the net rate of circulation flux. These bound vortices also travel upstream by the moving surface and disappearing. Alternate vortex shedding activity diminishes and completely disappears when $\lambda = 2.7$ resulting in the periodic Kármán vortex street suppression.

Acknowledgment

References

[1] Barnes, F.H. (2000). Vortex shedding in the wake of a rotating circular cylinder at low Reynolds number, *J. Physics*, Vol. 33, pp. 141.
[2] Massons, J., Ruiz, X. and Diaz, F. (1989). Image processing of the near wakes of stationary and rotating cylinders, *Journal of Fluid Mechanics*, Vol. 204, pp. 167.
[3] Tanaka, H. and Nagano, S. (1973). Study of flow around a rotating circular cylinder, *Bull. JSME*, Vol. 16, pp. 234.
[4] Swanson, W.M. (1961). The Magnus effect: A summary of investigations to date, *Journal of Basic Engineering*, Vol. 83, pp. 461.
[5] Diaz, F., Gavalda, J., Kawall, J.G., Keffer, J.F. and Giralt, F. (1983). Vortex shedding from a spinning cylinder, *Physics of Fluids*, Vol. 26, pp. 3454.
[6] Badr, H.M., Coutanceau, M., Dennis, S.C.R. and Menard, C. (1990). Unsteady flow past a rotating circular cylinder at Reynolds number 10^3 and 10^4, *Journal of Fluid Mechanics*, Vol. 220, pp. 459.
[7] Chang, C.C. and Chern, R.L. (1991). Vortex shedding from an impulsively started rotating and translating circular cylinder, *Journal of Fluid Mechanics*, Vol. 233, pp. 265.
[8] Chew, Y.T., Cheng, M. and Luo, S.C. (1995). A numerical study of flow past a rotating circular cylinder using a hybrid vortex scheme, *Journal of Fluid Mechanics*, Vol. 299, pp. 35.
[9] Dol, S.S., Kopp, G.A. and Martinuzzi, R.J. (2008). The suppression of periodic vortex shedding from a rotating circular cylinder, *Journal of Wind Engineering and Industrial Aerodynamics*, 96, pp.1164–1184
[10] West, G.S. and Apelt, C.J. (1982). The effects of tunnel blockage and aspect ratio on the mean flow past a circular cylinder with Reynolds number between 10^4 and 10^5, *Journal of Fluid Mechanics*, Vol. 114, pp. 361.
[11] Laneville, A. (1990). Turbulence and blockage effects on two dimensional rectangular cylinders, *Journal of Wind Engineering and Industrial Aerodynamics*, Vol. 33, pp. 11.
[12] Coleman, H.W. and Steele, W.G. (1989). *Experimental Uncertainty Analysis for Engineers*, Wiley, New York.
[13] Roshko, A. (1954). On the drag and shedding frequency of two-dimensional bluff bodies, *NACA TN* No. 3169.
[14] Zdravkovich, M.M. (1997). *Flow around circular cylinders: a comprehensive guide through flow phenomena, experiments, applications, mathematical models, and computer simulations, Vol. 1: Fundamentals*, Oxford University Press, Oxford, UK.
[15] Zdravkovich, M.M. (2003). *Flow around circular cylinders: a comprehensive guide through flow phenomena, experiments, applications, mathematical models, and computer simulations, Vol. 2: Applications*, Oxford University Press, Oxford, UK.
[16] Dol, S.S. (2004). *The suppression of periodic vortex shedding from a rotating circular cylinder*. M.E.Sc. Thesis. Western Ontario University, Ontario, Canada.
[17] Bailey, S.C.C., Kopp, G.A. and Martinuzzi, R.J. (2003). Vortex shedding from a square cylinder near a wall, *Journal of Turbulence*, Vol. 3, pp. 1.
[18] Saffman, P.G. and Schatzman, J.C. (1981). An inviscid model for the vortex-street wake, *Journal of Fluid Mechanics*, Vol. 122, pp. 467.